

Naval Research Laboratory

Washington, DC 20375-5000

2



NRL Memorandum Report 6456

Near-Neighbor Algorithms for Processing Bearing Data

J.M. PICONE, J.P. BORIS, S.G. LAMBRAKOS, J. UHLMANN* AND M. ZUNIGA**

*Center for Computational Physics Developments
Laboratory for Computational Physics and Fluid Dynamics (LCPFD)*

**Berkeley Research Associates, Springfield, VA 22150*

***Science Applications International Corporation, McLean, VA 22102*

AD-A207 935

DTIC
ELECTE
MAY 19 1989
S D D
C/S

May 10, 1989

REPORT DOCUMENTATION PAGE				Form Approved OMB No 0704-0188	
1a. REPORT SECURITY CLASSIFICATION UNCLASSIFIED		1b. RESTRICTIVE MARKINGS			
2a. SECURITY CLASSIFICATION AUTHORITY		3. DISTRIBUTION / AVAILABILITY OF REPORT			
2b. DECLASSIFICATION / DOWNGRADING SCHEDULE		Approved for public release; distribution unlimited.			
4. PERFORMING ORGANIZATION REPORT NUMBER(S) NRL Memorandum Report 6456		5. MONITORING ORGANIZATION REPORT NUMBER(S)			
6a. NAME OF PERFORMING ORGANIZATION Naval Research Laboratory	6b. OFFICE SYMBOL (If applicable) Code 4440	7a. NAME OF MONITORING ORGANIZATION			
6c. ADDRESS (City, State, and ZIP Code) Washington, DC 20375-5000		7b. ADDRESS (City, State, and ZIP Code)			
8a. NAME OF FUNDING / SPONSORING ORGANIZATION SDIO	8b. OFFICE SYMBOL (If applicable)	9. PROCUREMENT INSTRUMENT IDENTIFICATION NUMBER			
8c. ADDRESS (City, State, and ZIP Code) Washington, DC 20301-7100		10. SOURCE OF FUNDING NUMBERS			
		PROGRAM ELEMENT NO	PROJECT NO	TASK NO	WORK UNIT ACCESSION NO
11. TITLE (Include Security Classification) Near-Neighbor Algorithms for Processing Bearing Data					
12. PERSONAL AUTHOR(S) Picone, J.M., Boris, J.P., Lambrakos, S.G., Uhlmann,* J. and Zuniga,** M.					
13a. TYPE OF REPORT Interim	13b. TIME COVERED FROM 2/88 TO 2/89	14. DATE OF REPORT (Year, Month, Day) 1989 May 10	15. PAGE COUNT 49		
16. SUPPLEMENTARY NOTATION *Berkeley Research Associates, Springfield, VA 22150 **Science Applications International Corporation, McLean, VA 22102					
17. COSATI CODES		18. SUBJECT TERMS (Continue on reverse if necessary and identify by block number)			
FIELD	GROUP	SUB-GROUP	Near-neighbor algorithms Bearing data		
			Passive sensors Multisensor data fusion		
19. ABSTRACT (Continue on reverse if necessary and identify by block number)					
<p>The authors discuss the use of near-neighbor algorithms for correlating sets of tracks and sensor data on large numbers of rapidly moving objects. By investigating the scaling of such algorithms with the numbers of elements in the data sets, one finds that near-neighbor algorithms need not be universally more cost-effective than brute force methods. While the data access time of near-neighbor techniques scales with the number of objects N better than brute force, the cost of setting up the data structure could scale worse than</p> <p style="text-align: right;">(Continues)</p>					
20. DISTRIBUTION / AVAILABILITY OF ABSTRACT <input checked="" type="checkbox"/> UNCLASSIFIED/UNLIMITED <input type="checkbox"/> SAME AS RPT <input type="checkbox"/> DTIC USERS			21. ABSTRACT SECURITY CLASSIFICATION UNCLASSIFIED		
22a. NAME OF RESPONSIBLE INDIVIDUAL J.M. Picone			22b. TELEPHONE (Include Area Code) (202) 767-3055		22c. OFFICE SYMBOL Code 4440

Abstract

19. ABSTRACTS (Continued)

brute force by a multiplicative factor of $\log N$ in an extreme case. For cases in which near-neighbor algorithms are advantageous, the authors describe how such techniques could be used to correlate three-dimensional tracks with bearing data recorded as two angles (θ, ϕ) from a single sensor. The paper then presents a high-speed algorithm for fusing bearing data from three or more sensors with overlapping fields of view in order to obtain the three-dimensional positions of the objects being observed. The algorithm permits the use of near-neighbor techniques, reducing the scaling of the problem from N^m to $N \ln N$, where N is the number of objects in the common domain of observation, and m is the number of sensors involved. Numerical tests indicate the relative efficiencies of typical near-neighbor techniques in solving the multisensor angle-to-position fusion problem.

Keywords: PASSIVE SENSORS. (FC)

N to the m power

CONTENTS

I.	INTRODUCTION	1
II.	DATA CORRELATION IN MANY-BODY SCENARIOS	3
II.1	WHY NEAR-NEIGHBOR ALGORITHMS	4
II.2	WHEN WILL NN ALGORITHMS WORK BEST FOR TRACKING AND CORRELATION	7
III.	SINGLE SENSOR BEARING DATA	15
III.1	HOCKNEY'S METHOD	15
III.2	THE MONOTONIC LAGRANGIAN GRID [3.5]	17
IV.	THREE SENSORS WITH OVERLAPPING FIELDS OF VIEW	22
IV.1	TRANSFORMATION OF BEARING DATA TO NEW ANGLES	24
IV.2	REPRESENTATIVE ALGORITHMS AND TESTS	28
IV.3	PERFORMANCE RESULTS ON A SUN-260 WORKSTATION	31
IV.4	CONCLUSIONS FROM TESTS	35
IV.5	ESTIMATES OF PERFORMANCE ON OTHER HARDWARE	35
V.	SUMMARY	37
VI.	ACKNOWLEDGEMENTS	38
	REFERENCES	39
	APPENDIX — Details of Multisensor Bearing-to-Position Conversion	41

Accession For	
NTIS CR&I	<input checked="" type="checkbox"/>
DTIC TAB	<input type="checkbox"/>
Unannounced	<input type="checkbox"/>
Justification	
By _____	
Distribution/	
Availability Codes	
Dist	Avail and/or Special
A-1	



NEAR-NEIGHBOR ALGORITHMS FOR PROCESSING BEARING DATA

I. Introduction

One of the more pressing problems in Correlator-Tracker (CT) algorithms is the efficient use of sensor data consisting of only the bearings of objects relative to the sensor. By assumption, no range information is available, or the range is much less accurately known than the bearing. Infrared sensors will produce bearing data, for example. Here we present recent progress in processing and using such data. The paper emphasizes use of data structures designed for ready access of information on the near neighbors of each object, such as a track or contact report, within an ensemble. Implicit in the discussion is the perceived need for optimization on highly parallel or vector computers of the present and future in order to handle tens or hundreds of thousands of objects as rapidly as possible. The goal is to perform the same calculation simultaneously on large subsets of these objects.

Since the likelihood of association of a track with a sensor observation or "report" decreases with track-report separation, one usually assumes that rapid access of near neighbors will drastically reduce the work required in updating tracks through the use of new sensor data. The next section discusses the conditions under which the use of near-neighbor (NN) algorithms is actually advantageous. This discussion also indicates conditions under which the use of NN techniques might not be advisable. Section III then considers the correlation of bearing data with tracks in three-dimensional space. Section IV shows how to use bearing data derived from sensors with overlapping fields of view to determine the three-dimensional positions of the objects within the common domain of observation. Here the pivotal innovation is the reduction of the problem from enumerating the *intersections of bearing vectors* recorded by different sensors to evaluating the *equality of pairs of special angles* computed from the bearing data. This format facilitates the use of near-neighbor searches and fast sorting algorithms and vastly reduces the computer time required.

The reader should note that the term "track" might be used here in a less precise sense than the designers of correlator-tracker software might desire. Define the term "target

map" to be the statistical representation of a state vector at a given time for a possible object, as determined from sensor contact reports [1]. A track is then a time sequence of target maps corresponding to the same object. The statistical nature of the target map derives from errors implicit in the measurement and estimation process. To determine near neighbors in the present paper, the authors use the mean locations (or expectation values of the respective positions) of the contact reports and target maps. Further, the term "track" stands for the mean location of the target map at a given time t .

II. Data Correlation in Many-Body Scenarios

In this discussion, a data set will contain "data elements," each of which corresponds to one of a set of objects being observed. Thus each data element can be a contact report from one of an array of sensors covering a region of physical space or a target map produced by a correlator-tracker from such data. The statement that two data elements are "correlated" means that each data element describes or pertains to the same physical object with a likelihood that exceeds some threshold value. The statement that two disjoint sets of data elements are "related" means that each of the sets contains at least one data element that is correlated to a data element of the other.

The problem considered here is stated as follows: given $M \geq 2$ related, disjoint sets of data (denoted S_1, S_2, \dots, S_M), find the elements of the respective sets which are correlated with each other. That is, find all sets $\{a_i, b_j, \dots, c_m\}$ where $a_i \in S_1, b_j \in S_2, \dots$, and $c_m \in S_M$, so that a_i, b_j, \dots, c_m are all correlated. "Data correlation" or simply "correlation" is the process of identifying correlated data elements. In practice, the determination that two elements of different data sets are correlated can be approximate (probability of correlation less than one), and estimating the degree of correlation requires the calculation of a *correlation score*. As indicated above, one example is the act of finding the track (constructed from previous data) which is correlated with a new sensor contact report. Upon establishing this relationship, one can extend the track to later times, using the new contact report to refine the track.

The relevant scenarios comprise tens to hundreds of thousands of rapidly moving objects. We further assume that the period under consideration is a few hours at most. Because of the large numbers, high speeds and short time scales involved, time delays of even a minute in data processing could be too large to react to the situation. One thus immediately concludes that data correlation in this case requires highly parallel computers with large amounts of memory, so the requisite data processing can be as nearly instantaneous as possible. Only analysis and numerical simulations of realistic scenarios

containing such large numbers of objects can provide estimates of the computing needs in this situation.

II.1 Why Near-Neighbor Algorithms?

Work has begun on the development of highly parallel correlation algorithms under the assumption that scalar algorithms and hardware would not be adequate for the scenarios mentioned above. The parallel environment would permit groups of correlation calculations to be performed simultaneously. Ideally the individual data elements involved in the parallel calculation correspond to the same observation time or nearly the same observation time t_0 . This is where near-neighbor algorithms offer the greatest advantage over brute force methods.

A "brute force" method computes a correlation score for all possible sets $\{a_i, b_j, \dots, c_m\}$. When the data sets S_1, S_2, \dots, S_M , contain the same number of elements $N_1 = N_2 = \dots = N_M \equiv N$, the brute force calculation scales as N^M , where M is the number of data sets to be correlated at one time. This paper considers problems for which $M = 2$ or 3 .

A "near-neighbor" algorithm is a method for storing and accessing data on N objects so that the following conditions hold:

- (1) Storage and access of data depends on object parameters: for example, position, velocity, or attributes. In a dynamical system, time can either be explicit or implicit in the near-neighbor data structure.
- (2) The storage and access depend on indexing the data or pointers to the data (a "data structure") so that the indices themselves contain information on parameter values; and
- (3) On average, scaling of the access time with N is better than "brute force" methods by a factor of approximately $N/\log N$ or better.

Near-neighbor algorithms eliminate an appreciable fraction of the combinations $\{a_i, b_j, \dots, c_m\}$ from consideration before correlation scores are computed. Consider

the case $M = 2$. For each $a_i \in S_1$, one accesses only the data elements in S_2 which satisfy definite criteria for being near neighbors of a_i . The resulting subset of S_2 is $NN_{21}(i) \equiv \{b_j | b_j \text{ NN of } a_i\} \subset S_2$ and the correlation score is computed only for the near neighbors $NN_{21}(i)$. Depending on the particular NN algorithm, the cost of accessing near neighbors for each $a_i \in S_1$ scales as either N^0 (constant) or $\ln N$. So the cost for N such calculations (all elements of S_1) scales as N or $N \ln N$, both of which are less than brute force scaling. For $N = 10,000$ objects and $M = 2$, the use of NN algorithms gives a potential improvement of three to four orders of magnitude over the brute force approach. For $M = 3$, the improvement can be seven to eight orders of magnitude.

To summarize the above discussion, a near-neighbor algorithm involves the construction and use of an intermediate data structure which permits the rapid identification of likely candidates (usually a relatively small number) for correlation with a given data element before the actual correlation score calculation is done. If the same near-neighbor data structure is used for all data accesses, the scaling with N , the number of elements in a data set, is faster by several orders of magnitude than is a brute force algorithm, when N is large.

Table 1 lists near neighbor algorithms that the authors have developed or tested. The quantity N is the number of elements of set S_1 , all of which reside in the near-neighbor data structure. Column 2 shows the scaling of the time required to set up the NN data structure. The scaling of the cost for accessing near neighbors of a given element of S_1 appears in the third column. For this operation, NN algorithms are superior to brute force. On the other hand, column 2 indicates that if only a few accesses occur before the data structure must be set up again or reconstructed, the total cost of using a near neighbor algorithm could scale more poorly with N than brute force. The NN algorithm is not necessarily optimal in every case. For use of a NN algorithm to be beneficial, the cost of organizing the data according to a NN data structure and computing scores for the resulting limited subsets of $S_1 \otimes S_2$ must be less than the total cost (over the entire set S_2) of comparing all elements b_j of S_2 with all elements a_i of S_1 .

Table 1 — Scaling of Candidate Gating Algorithms

<u>ALGORITHM</u>	<u>SETUP</u>	<u>SCALING*</u> \Rightarrow	<u>ACCESS</u>	<u>MEMORY</u>
Hypercube Flashing	N	1	1	N
Hockney Cells	N	1	1	N
MLG [†]	N lnN	1	1	N
Ordered Partition	N lnN	\leq lnN	\leq lnN	N
BLD [†] Tree	N lnN	lnN	lnN	N
Brute Force	0	N	N	N

* Coefficients can vary considerably

† Monotonic Lagrangian Grid

‡ Bilinear Decomposition

II.2. When Will NN Algorithms Work Best for Tracking and Correlation?

To see how NN algorithms can increase the speed of data correlation, one can analyze the following equation for the cost in computer time of correlating all N_2 elements of set S_2 with all N_1 elements of S_1 :

$$C = C_n + C_s . \quad (2.2.1)$$

In Eq.(2.2.1), C_n is the cost of finding the elements $b_j \in S_2$ which are near neighbors of the respective $a_i \in S_1$; and C_s is the time required to compute scores for all of the NN pairings $\{a_i, b_j\} \in NN_{21}(i)$, for $i = 1, 2, \dots, N_1$. The scaling of each term with N_1 and N_2 provides a basis for initial comparison of NN algorithms with brute force methods. The constant coefficients multiplying the scaling functions will vary with the computer hardware and the degree to which the software is optimum for that hardware.

In the context of correlation and tracking, define set S_1 as the set S_R of contact reports, corresponding in the most general case to different observation times $\{t_i ; i = 1, 2, \dots, N_r\}$, where $N_1 \equiv N_r$, the number of contact reports. The set S_2 is then equal to S_T , the set of $N_2 \equiv N_t$ tracks. Thus for each contact report $a_i \in S_1$ our objective is to identify all tracks in S_2 that are correlated with a_i . The tracks in S_2 all correspond to the same time t_j , which is different from the observation times for the set $\{a_i\}$ in the most general case. The computation of a correlation score requires that a track and a report correspond to the same time [2], so that, in theory, the set of tracks must be extrapolated to the time corresponding to each contact report $a_i \in S_1$. The score can decrease on average with track-report distance, but is not, in general, a function of the distance alone.

II.2.1. "Brute Force" Methods

A brute force method treats each contact report separately from the others and performs calculations (not necessarily scores) for all possible pairings of tracks with contact reports. Several brute force procedures are possible. Below we assume that extrapolation of each track to the time of each report is implicit in any brute force algorithm.

Procedure 1. For each contact report a_i , compute the "distances" D_{ij} to all tracks b_j . For each track satisfying $D_{ij} \leq R$, where R is a distance chosen to define near neighbors, compute the correlation score. The scaling of the cost equation (2.2.1) with N_r and N_t is

$$C_1^b = A_{1a}^b N_r N_t + A_{1c}^b N_r . \quad (2.2.2)$$

In this equation, the coefficients A are constant, and the superscript b signifies "brute force." The coefficient A_{1c}^b depends on the average number of tracks found to be near neighbors of each contact report and the cost of computing a score. Because the first step of Procedure 1 culled out the tracks that were poor candidates for correlation, the second term does not depend on N_t . The coefficients are important, since the actual correlation calculation will be much more expensive than the calculation of distances in the first step. Notice that the distances D_{ij} are straightforward to calculate only when physical positions are used to define "near neighbors". If other attributes are to be considered, the testing might be on intervals of attribute values rather than on a normalized "distance" function.

A possible drawback of Procedure 1, as described above, is that the value of R is somewhat arbitrary and in fact might have to be inefficiently large to ensure finding all the correlations with acceptable scores. The reason is that the score is not a function of R alone, additionally depending on the statistical distributions defining the track state vector and the contact report. This means that some tracks with unacceptable correlation values would be selected in the near-neighbor-access step of Procedure 1. Alternatively one could do a simple comparison to find all tracks within an initial radial interval $(0, R_0)$ of contact report a_i and compute scores for this subset $NN_{21}(i)$. Then choose a radius $R_1 > R_0$. For the remainder of the tracks (the set $S_2 - NN_{21}(i)$), find the tracks in the interval (R_0, R_1) , compute their correlation scores, and eliminate those tracks from the set of candidates for the next radial interval. This process continues to larger distances R_l until all correlation scores for the tracks in the interval (R_l, R_{l+1}) fall below a selected threshold. The size of the subset of S_2 to be searched and the associated cost decrease

with successive radial intervals. In addition the algorithm should identify all correlations with a score above the threshold. Testing on realistic scenarios is necessary to determine the efficiency of Procedure 1 relative to the procedures below.

Procedure 2. For each contact report a_i , compute the full correlation score for all tracks. Keep only those tracks with scores above some minimum acceptable value or threshold. The scaling of the cost equation (2.2.1) with N_r and N_t is

$$C_2^b = A_{2c}^b N_r N_t . \quad (2.2.3)$$

Here no preliminary determination of near neighbors has occurred before the correlation score calculation, so that Eq.(2.2.3) indicates greater cost than both parts of the previous procedure, given that calculating the correlation score is the most expensive part of the algorithm.

Procedure 3. For each contact report a_i , compute and sort the distances D_{ij} to all tracks, and compute correlation scores in order of increasing distance until the score falls below a minimum acceptable value. The cost of this is harder to quantify because the number of scores calculated depends on a score threshold instead of a distance threshold. A useful equation is

$$C_3^b = A_{3n}^b N_r N_t + A_{3n}^{b'} N_r N_t \ln N_t + A_{3c}^b f N_t N_r . \quad (2.2.4)$$

The coefficient A_{3c}^b depends on the cost of computing a score. The quantity f is the average fraction of the N_t tracks for which correlation scores must be calculated on a "per contact report" basis. If f is sufficiently small, this procedure should cost less than Procedure 2. In addition, if $f \sim N_t^{-\alpha}$, where $\alpha > 0$, then the scaling of the score calculation (third term) is better than in Eq.(2.2.3). This method also eliminates the potential drawback of Procedure 1 that the value chosen for R is somewhat arbitrary and in fact might have to be chosen undesirably large to ensure finding all the correlations with acceptable values.

Notice that the first two terms have potentially more expensive scaling than the third but that the coefficients A_{3n}^b and $A_{3n}^{b'} \ln N_t$ could be much smaller than $A_{3c}^b f$. In addition, the remote possibility exists that, even for large numbers of objects, the coefficients A could be more important than the scaling with N_r and N_t .

Procedure 4. Here we mention a nonhierarchical cluster algorithm [1], which is discussed in a companion document [3] and analyzed fully there. This algorithm identifies and uses clusters containing tracks and reports which can only be associated with members of the cluster in which they reside. Based on this information, the computation of correlation scores has scaling ranging between $N^{3/2}$ and N^2 , depending almost entirely on the scenario. We refer the reader to the above reference [3] for further information.

An important factor in the values of the coefficients for the above procedures is the availability and type of computer hardware. The speed-up through parallelization and the parallel implementation itself will likely vary with the particular calculation (each term in the above equations). This could change the scaling with N in the cost equations or change the relative importance of the individual terms. In addition, for particular multiple-hypothesis-tracking (MHT) algorithms, some of the procedures above might not be possible or acceptable. Most importantly for the brute force algorithms, the processing of each contact report will be the same whether the contact report time stamps $\{t_i\}$ are different or not. This could result in an advantage over near-neighbor algorithms, which are considerably more efficient when many of the contact reports have approximately the same time stamps.

II.2.2 Near-Neighbor (NN) Algorithms

As indicated earlier, NN Algorithms are best suited for processing groups of contact reports in a parallel or vector fashion. The constraints on the operational sensor system itself can limit the utility of such algorithms, for example, when only a few objects are being tracked or when the sensor produces reports corresponding to different times. At least three cases occur in correlator-tracker problems:

Case 1. Appreciable numbers of contact reports in S_R correspond to approximately the same observation time t_o . In this case, the same near-neighbor data structure containing the tracks extrapolated to $t_j = t_o$ can be used to process those contact reports. Then the cost equation is

$$C_1^n = A_{1n}^n N_t \ln N_t + A_{1c}^n N_r \quad (2.2.5)$$

or

$$(C_1^n)' = (A_{1n}^n)' N_t + (A_{1c}^n)' N_r, \quad (2.2.6)$$

depending on the scaling of the cost for setting up the NN data structure. Notice that in either case, the scaling with N_r and N_t is superior to the brute force methods. Case 1 applies best when the range of contact report observation times is comparable to or smaller than the minimum time for any track to overtake another, thus disturbing the NN data structure.

Table 2 shows timings for some of the data structures in Table 1 on a SUN 260 (scalar) workstation for the case that all of the contact reports have the same time stamp. These tests distributed 8K sizeless points, designated "tracks," and 8K additional sizeless points, designated "reports," over a three-dimensional space uniformly and randomly. The " k -d tree" is a standard k -dimensional binary tree structure and search; in this case, $k = 3$. The various methods then found the five nearest tracks for each report. We see that near-neighbor algorithms provide a tremendous advantage over brute force algorithms when Case 1 applies.

Case 2. The other end of the spectrum is the situation in which the reports correspond to a wide range of observation times, all widely separated from each other. To determine likely track-report pairings, the set of tracks might have to be extrapolated to each different contact report time t_i . The NN data structure containing the tracks might then have to

Table 2 — Preliminary Tests of Candidate Gating Algorithms

<u>ALGORITHM</u>	<u>SCALING</u>	<u>SETUP(s)*</u>	<u>ACCESS(s)*</u>	<u>ACCURACY(%)</u>
MLG	N lnN	4.4	82.0	99.7
MLG/ORDERED PARTITION	N lnN	2.3	13.8	100
BLD TREE#	N lnN	1.9	10.4	100
K-D TREE	N lnN	2.0	12.1	100
HYPERCUBE HASHING	N	2.5	23.2	100
BRUTE FORCE	N ²	0	7000	100

* COSTS MEASURED IN CENTRAL PROCESSOR SECONDS

BILINEAR DECOMPOSITION (NEWLY DEVELOPED AT NRL)

be set up anew for each report. Given that this happens approximately N_r times, the cost is

$$C_2^n = A_{2n}^n N_r N_t \ln N_t + A_{2c}^n N_r \quad (2.2.7)$$

or

$$(C_2^n)' = (A_{2n}^n)' N_r N_t + (A_{2c}^n)' N_r \quad (2.2.8)$$

Assuming that $N_r \sim N_t \sim N$, the actual number of objects, comparison with the earlier equations for brute force methods shows that *in this case* the scaling for NN algorithms is no better or even worse than brute force. Thus if the contact reports are processed one at a time and the observation times are all sufficiently different, NN algorithms might not provide an advantage over brute force algorithms.

Case 3. An intermediate situation prevails if the various objects change their indices in the NN data structure slowly with time. This means that their *relative positions* in parameter space remain the same over appreciable periods of time. The NN data structure then remains the same for a range of contact report observation times and accessing the near-neighbors of a contact report can proceed as in Case 1. Of course, the actual spatial coordinates associated with a given set of indices in the NN data structure do change and one must account for this change in values when accessing near neighbors. Methods of doing this are presently under development by the authors (e.g., [3]).

Note that, as in Brute Force Procedure 1, the distance R or the parametric intervals used to define the concept of "nearness" might have to be larger than optimum to assure the user of finding all candidate pairs with correlation scores above some threshold. The choice of R might be somewhat arbitrary, and because the problem is inherently statistical, the chance of missing a required candidate on the first pass is still nonzero. This depends on the form of the scoring function. As in brute force Procedure 1, making a sequence of

near-neighbor search and scoring procedures at succesively larger radius might overcome the limitation:

- (1) Using a near-neighbors data structure, find the tracks with $D_{ij} \leq R_0$, for some reasonable R_0 and compute scores. Record all of the tracks (subset $NN_{21}(i)$) found in this step.
- (2) Using the same data structure and a larger radius R_1 , find the tracks with $R_0 < D_{ij} \leq R_1$ in the reduced set $S_2 - NN_{21}(i)$. Compute scores and compare to the threshold. Eliminate the tracks found in this step from the subset of tracks subjected to subsequent searches.
- (3) Repeat step (2) in the interval $(R_1, R_2]$. Continue this procedure for subsequent contiguous intervals until all scores in an interval fall below the threshold.

III. Single Sensor Bearing Data

The discussion below considers cases in which three-dimensional tracks are to be correlated with the two-dimensional bearing data. Figure 1 depicts this situation. The black dots are the centra of the various "target maps" at the present time. Target maps represent (statistically) the state vectors of potentially real objects at a given time t . Tracks are then time sequences of target maps, each sequence corresponding to a presumed physical object. Because tracks are derived from incomplete data and are subject to ambiguous interpretations, more tracks will usually exist than actual objects. As indicated earlier, we sometimes use the terms "track" and "target map" interchangeably for convenience.

The coordinate axes at the left side of Fig. 1 are symbolic of any universal coordinate system in which the tracks are defined. The vector S defines the location of the sensor in this coordinate system. Because the range of the contact reports is assumed to be unknown, bearing data from a single sensor could be correlated with any targets lying within a cone, whose vertex lies at the position of the sensor and whose solid angle corresponds to the angular resolution of the sensor. In the figure, $(\Delta\theta_s, \Delta\phi_s)$ define the allowed angular interval for correlation of tracks with a contact report at the spherical coordinates (θ_s, ϕ_s) .

In this section, the number of dimensions of the parameter space defining near neighbors is $n = 2$, corresponding to (θ, ϕ) , and the data arrays in computer memory will be two-dimensional. Picone *et al.* [3] discuss examples of such schemes, two of which are described in the following subsections.

III.1. Hockney's Method

In Hockney's method [4], an n -dimensional rectangular grid overlays the physical space containing the tracks and contact reports. Each side of a rectangular cell corresponds to one of the physical parameters defining the correlation calculation (e.g., spatial coordinates, velocity components, or physical attributes of the objects being tracked) and has length L_i . In the present case, l is one of the angular spherical coordinates centered on the sensor

$(\theta$ or $\phi)$ and $n = 2$. To find which rectangle contains a given point, (θ_i, ϕ_i) requires two multiply operations

$$(I_i, J_i) \equiv \left(\left[\theta_i \times \frac{1}{L_\theta} \right], \left[\phi_i \times \frac{1}{L_\phi} \right] \right), \quad (3.1)$$

where (I_i, J_i) are the indices of the cell in which object i is located and the brackets $([a])$ indicate the greatest integer less than or equal to the quantity a . To handle cells containing more than one object, one employs linked lists. Thus the near neighbors of a given object are those within the same cell and the adjacent cells. The cost of partitioning the objects among the cells according to Eq.(3.1) scales as N_t , the total number of tracks. This method permits parallel calculations of correlation scores, but should not permit vectorization on a Cray computer. Because the indexing of the objects in memory bears a direct relationship to the actual (not relative) values of the parameters (θ, ϕ) for each object, this method will permit the user to find all of the near neighbors corresponding to a given correlation radius R_c . For nonuniform distributions of objects, many cells could be empty. In addition, the values of L_θ and L_ϕ are somewhat arbitrary. Both factors could cause wasted memory, and the latter could lead to inefficiency and total costs for correlation which scale more expensively than Eq.(2.2.6) would indicate. In parallel processing, load balancing becomes a concern because some nodes can have many neighbors while others may have none.

III.2. The Monotonic Lagrangian Grid [3, 5]

The Monotonic Lagrangian Grid (MLG)* correlator could be based on (θ, ϕ) in a spherical coordinate system having its origin ($r = 0$) at the position of the sensor. The MLG would then be a two-dimensional data structure containing both the bearings of the target maps relative to the sensor and the new bearing contact reports. The pairs $(\theta(i, j), \phi(i, j))$ would have a "monotonic" order in the sense that

* Early papers used the term "Monotonic Logical Grid" for this data structure.

$$\theta(i, j) \leq \theta(i + 1, j)$$

$$\phi(i, j) \leq \phi(i, j + 1) .$$

Then, according to the simplest concept, the identification of potential correlations would only require computing scores of target maps lying within index neighborhoods of the contact reports. The ordered partition of Kim and Park [6] provides a way to augment an MLG so that a tree search can be performed.

The calculation of the MLG indices would proceed precisely as in the Cartesian case [3]. Transformation of the target maps from some universal coordinate system to the (r, θ, ϕ) sensor system would require only highly parallel and vectorizable calculations *which would also be necessary for any non-MLG technique!* This process scales as order (N_t) or order (1), depending on the computer architecture and memory and the number of target maps to be processed. For scalar, MIMD (multiple instruction stream, multiple data stream) or pipeline architectures, the MLG bearing data structure might consist of only pointers to the 3D MLG target map data array/file and the sensor contact report array/file. Thus the contact reports and target maps need not be stored twice. For SIMD (single instruction stream) architectures, actually combining and storing the data in a contiguous region of memory might be optimal.

Because the MLG is determined primarily by the relative locations of the target maps and *not* the origin of the coordinate system, the motion of the sensor should not have much of an effect on the structure of the MLG. Only local swaps of the target maps in the data structure would be necessary to maintain the MLG over the time interval during which new sensor data are processed, if this is at all necessary. Our studies have shown such restructuring to be very fast. In passing, we note that the motion of the sensor relative to another (universal) coordinate system would not affect the speed of transformation of spatial coordinates from one system to the other. This is so because the motion merely changes the value of the vector S relating the origins of the two systems.

A drawback to the MLG for CT problems is that the storage of data in computer memory can result in local distortions of the relative configuration of objects in physical space. If the same index offsets are used to access the tracks that are near neighbors of each contact report, some of the near neighbors can be missed if these index offsets are chosen to be too small. Thus large index offsets might be necessary in dense regions to insure that all of the desired neighbors are found. This would mean that many undesirable candidates would be found as well, increasing the number of correlation calculations above the optimum level. This reflects a corresponding situation of many contact reports in a single cell of the Hockney data structure or many empty cells, if the cells are small. Apparently some information about the actual parameter values corresponding to MLG indices would be necessary to improve MLG performance under such conditions. This is the essence of the k -nearest neighbor finding algorithm of Kim and Park [6], which can be combined with an MLG data structure.

We assume that the reports all correspond to approximately the same time t_0 . If this is not the case, one might still be able to use the procedure given below with adjusted values of $\Delta\theta$ and $\Delta\phi$, the angular uncertainties in the observations (step 3). An outline of the MLG algorithm is as follows:

- (1) If necessary, compute the positions of the target maps (T_i) relative to the location of sensor S and corresponding to the time t_0 at which the observations took place. Derive (θ_i, ϕ_i) for each map T_i . Referring to Fig. 1, one obtains the position of track i :

$$\mathbf{R}_{,i} = \mathbf{R}_i - \mathbf{S}, \quad (3.2.1)$$

where

$$\mathbf{R}_{,i} \rightarrow (r_i, \theta_i, \phi_i). \quad (3.2.2)$$

(2) Define a convenient 2D MLG containing all (N_r) contact reports received from sensor S and the angular coordinates of all (N_t) candidate target maps at the corresponding time t_0 . Here the subscript "t" signifies "tracks." Ideally, the product of the dimensions N_i and N_j of the MLG would equal the total number of angle pairs $N_r + N_t \equiv N_{rt}$. However, N_{rt} might not be factorizable into the MLG dimensions desired (see text below). In Eq.(3.2.3) below, we, therefore, allow for the addition of ΔN "holes" to make up this difference. A hole is an element of the MLG which has specific, convenient values of (θ_h, ϕ_h) , but does not correspond to a track or a report. The MLG data structure thus contains the set

$$M_2 \equiv \{(x_{jk}, y_{jk}) | (x_{jk}, y_{jk}) \in \{(\theta_i, \phi_i)\} \cup \{(\theta_s, \phi_s)\} \cup \sum_h^{\Delta N} \Xi(\theta_h, \phi_h);$$

$$x_{jk} \leq x_{(j+1)k}, y_{jk} \leq y_{j(k+1)}\} . \quad (3.2.3)$$

(3) Search appropriate index neighborhoods of sensor bearing contact reports $\{(\theta_s, \phi_s)\}$ for sufficiently correlated target maps. The degree of correlation may be defined by the requirements that

$$|\theta_s - \theta_i| \leq \Delta\theta_{rt}$$

$$|\phi_s - \phi_i| \leq \Delta\phi_{rt} \quad (3.2.4)$$

where $\Delta\theta_{rt}$ and $\Delta\phi_{rt}$ are measures of the angular resolution of the sensor or a similar factor defining the required degree of agreement between contact reports and track bearings.

Item (2) above includes the possibility that M_2 would require a few more (ΔN) elements than N_{rt} in order that the total number of elements N_M is factorizable in the desired manner. For example, suppose we define the two dimensions of M_2 by

$$N_j = N_k \equiv [\sqrt{N_{rt}}] + 1, \quad (3.2.5)$$

where $[x]$ signifies the greatest integer less than x . Then the quantity

$$\Delta N = N_j^2 - N_{rt} \quad (3.2.6)$$

is the extra number of empty memory locations or "holes" within M_2 . In this case the holes are just a convenience in setting up the MLG and need not participate in the correlation calculation. Choosing hole locations in regions with a statistical paucity of real data might appreciably regularize the MLG structure.

IV. Three Sensors with Overlapping Fields of View

When one has multiple sensors with overlapping fields of view, the bearing data can provide enough information to derive the positions of the objects being observed without reference to tracks. The larger the number of sensors involved, the fewer will be the pathological cases for which ambiguous results are obtained. In the brute force approach, the bearing data may be represented graphically as rays (or cones) radiating from each sensor, and the intersections represent possible positions of objects being observed. For m_s sensors and N_r contact reports per sensor, checking the contact reports sequentially for intersections is very expensive from a combinatorial point of view, scaling approximately as $N_r^{m_s}$.

A method for finding these intersections (correlations) based on near-neighbor or sorting techniques, however, scales as $N_r \ln N_r$, which is a major improvement over brute force for $m_s = 3$ or higher. Using highly parallel computer architectures could cut this scaling by a factor of N_r . This section describes such an approach for the problem of three sensors, each of which provides bearing data only. Our interest is in the objects being observed in a region of space viewed by all three sensors. (As this report was going to press, the authors received information indicating that the algorithm presented below was developed earlier by R. Varad and perhaps others [7]. We requested reprints of the papers in question but have not yet received them to confirm the prior claim.)

Figure 2 shows a schematic diagram of this problem. The three sensors, labelled by A , B , and C , produce sets of contact reports that are subscripted respectively by a , b , and c , and labelled respectively by i , j , and k . Originally the reports give the spherical angles (θ, ϕ) defining a bearing vector, denoted by $e_{\alpha\beta}$, relative to a specific sensor. The subscript α gives the sensor identification while β labels the particular contact report produced by sensor α . Equation (4.1) represents this progression:

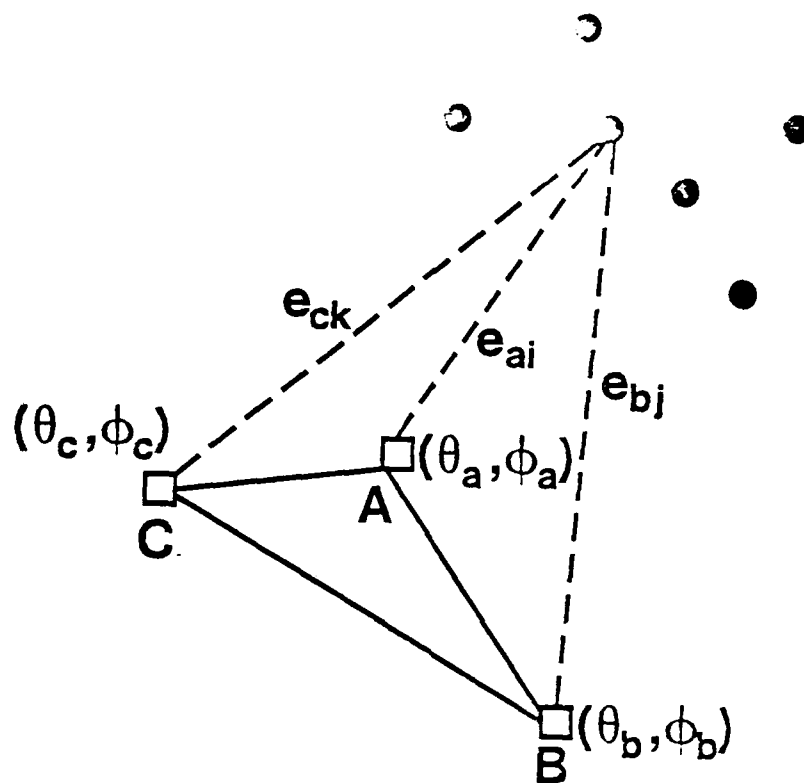


Fig. 2 — Conversion of bearings, produced by multiple passive sensors with a common field of view, to three-dimensional positions. The sensors are labelled *A*, *B*, and *C*, and the objects being observed are represented by black circles.

$$\begin{aligned}
A: \quad \mathbf{e}_{ai} &= (\theta_a(i), \phi_a(i)); \quad i = 1, 2, \dots, N_a \\
B: \quad \mathbf{e}_{bj} &= (\theta_b(j), \phi_b(j)); \quad j = 1, 2, \dots, N_b \\
C: \quad \mathbf{e}_{ck} &= (\theta_c(k), \phi_c(k)); \quad k = 1, 2, \dots, N_c
\end{aligned} \tag{4.1}$$

For the purpose of discussion, assume that the sensors produce exact bearing data. Then, as Fig. 2 shows, an object observed by all three sensors will reside at the intersections of the bearing vectors \mathbf{e}_{ai} , \mathbf{e}_{bj} , and \mathbf{e}_{ck} , for specific values of i , j , and k . Notice that the indices i , j , and k , corresponding to a threeway intersection, also provide unique labels for the physical object. As indicated above, the number of possible intersections is the product $N_a \times N_b \times N_c$ or N^3 , if $N_a = N_b = N_c \equiv N$. Because this scaling produces a "combinatorial explosion" as the number of contact reports increases, a better method of correlating the sensor data is necessary to derive positions for the objects being observed. The following discussion describes such a method.

IV.1. Transformation of Bearing Data to New Angles

Our solution of this problem is to convert the spherical coordinates (θ, ϕ) to two new angles which define the planes in which the bearing vectors $\{\mathbf{e}_{ai}\}$ lie relative to the plane containing the three sensors. A further assumption then is that the locations of the three sensors are also known.

For the purpose of introducing the method, our discussion does not include the angular resolution of the sensors. Errors in the angular data produced by the sensors translate into errors in the new angles resulting from the transformation. The Appendix presents a practical implementation of the ideas presented here and discusses effects of sensor resolution. The next subsection on practical algorithms and tests includes a simple representation of the angular error. Another ingredient of errors in the angles is differences in observation times of the contact reports produced by the sensors. Here we do not compute the effects of differences in "time stamps" of the reports.

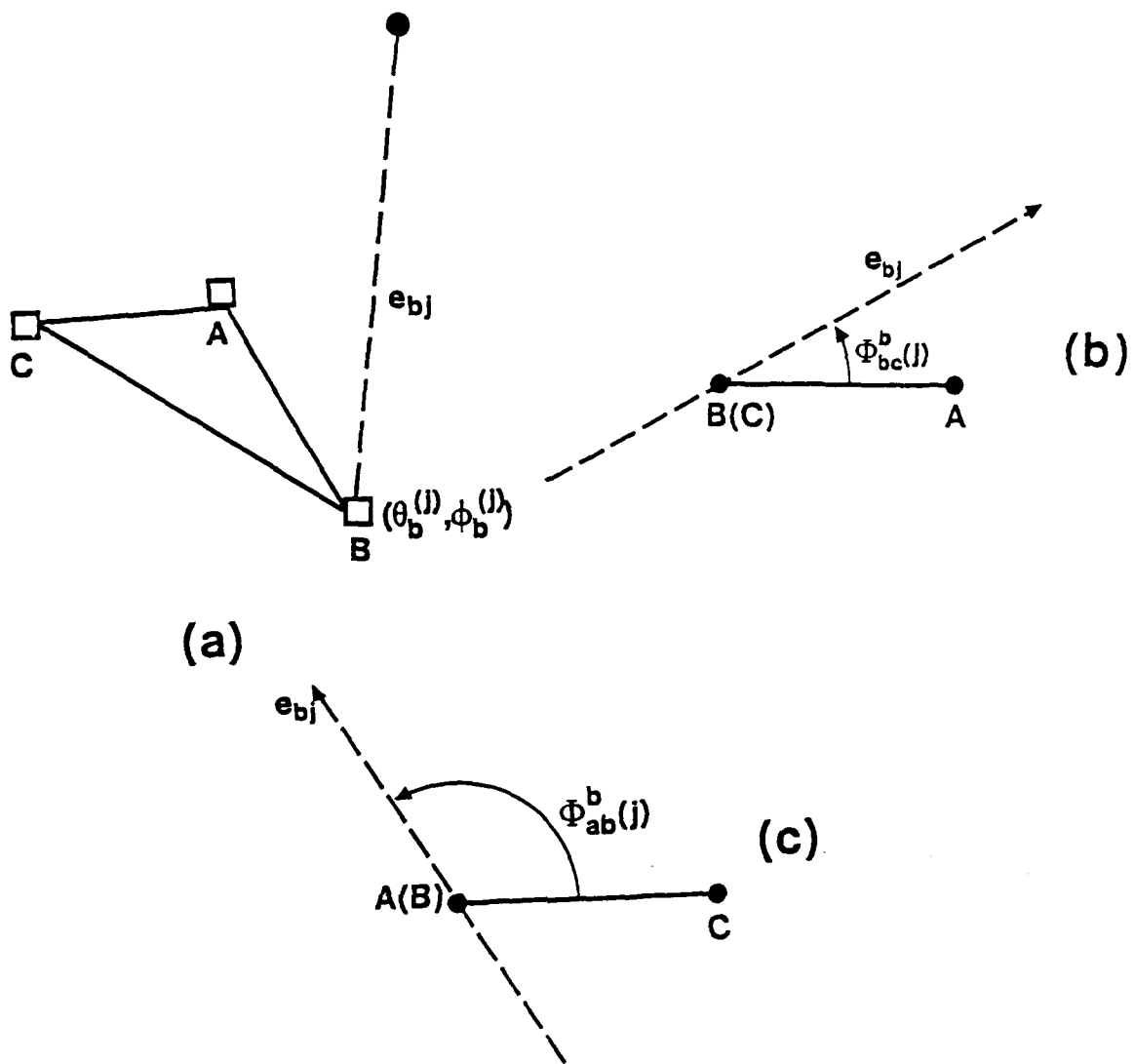


Fig. 3 — Conversion of the bearing angles $(\theta_b(j), \phi_b(j)) \equiv e_{bj}$, corresponding to observation j by sensor B , to new angles $\Phi_{bc}^b(j)$ and $\Phi_{ab}^b(j)$. The new angles correspond to the planes defined by the combination of e_{bj} with each of the lines between sensor B and the other sensors. Notice that the lines of sight for defining the angles are from sensor B toward sensor C and from A to B , according to the convention in Section IV.1 of the text. The sensor whose letter is in parentheses is hidden from the observer by the other sensor.

Now consider the bearing vector e_{bj} for report j of sensor B . This situation is reproduced in Fig. 3a, without the other objects and bearing vectors in Fig. 2. Notice in Fig. 3a that the bearing vector e_{bj} in combination with the vector e_{bc} along the line joining sensors B and C defines a unique plane. Similarly e_{bj} in combination with e_{ab} defines another unique plane. Further, these planes intersect at the bearing vector e_{bj} , so that knowledge of the planes is equivalent to the knowledge of the bearing vector.

The next step is to define each of the above planes in terms of a unique angular coordinate. Figures 3b and 3c indicate how this is done. Figure 3b shows the situation as viewed by an observer whose line of sight lies in the plane of the sensors and is directed along the line connecting sensors B and C (vector e_{bc}). The plane of the sensors appears as a horizontal line to the observer. The line connecting B and C appears to the observer as a point at the location of sensor B . The plane \overline{BCj} defined by the bearing vector e_{bj} and the vector e_{bc} appears as a line intersecting the plane of the sensors. The angle of rotation $\Phi_{bc}^b(j)$ between the plane \overline{BCj} and the plane \overline{ABC} containing the sensors is unique and thus defines the plane \overline{BCj} . Now view the same system along the line from sensor A to sensor B ; the observer sees the situation depicted in Fig. 3c. In the same manner, the angle $\Phi_{ab}^b(j)$ uniquely defines the plane \overline{ABj} .

This method has thus converted the angles $(\theta_b(j), \phi_b(j)) \equiv e_{bj}$ to two new angles $(\Phi_{bc}^b(j), \Phi_{ab}^b(j))$. The new angles correspond to the planes defined by the bearing vector e_{bj} and the lines joining sensor B with the other two sensors. These planes intersect to form the bearing vector e_{bj} . The same procedure performed on all bearing vectors from sensor A provides the set $\{(\Phi_{ab}^a(i), \Phi_{ca}^a(i)); i = 1, 2, \dots, N_a\}$, and similarly, the bearing vectors from sensor C provide the set $\{(\Phi_{bc}^c(k), \Phi_{ca}^c(k)); i = 1, 2, \dots, N_c\}$. By convention, the observer views the system in the plane and parallel to the lines joining pairs of sensors as follows:

- (1) For sensors A and B , along the direction from A to B ;
- (2) For sensors B and C , along the direction from B to C ; and

(3) For sensors A and C , along the direction from C to A .

This maintains a cyclic order among the triplet $A - B - C$. The index i , j , or k and the bold superscript a , b , or c , respectively, tells us which sensor has produced a given angle Φ in the above sets.

Now return to Fig. 2 and the case in which all three sensors have observed the same object. Let us assume that the bearing vectors e_{ai} , e_{bj} , and e_{ck} intersect at the location of an object as shown. First consider e_{ai} and e_{bj} . Because the two vectors intersect, they lie in the same plane. Further the line \overline{AB} also lies in the same plane. Thus the plane \overline{ABi} corresponding to angle $\Phi_{ab}^a(i)$ (derived from sensor A) is equivalent to the plane \overline{ABj} corresponding to angle $\Phi_{ab}^b(j)$ (derived from sensor B). The condition that the bearing vectors e_{ai} and e_{bj} correspond to the same object (i.e., that the vectors intersect) is thus

$$\Phi_{ab}^a(i) = \Phi_{ab}^b(j) \quad (4.1.1a)$$

Similar reasoning for the bearing vectors from the other pairs of sensors $B - C$ and $A - C$ gives us the conditions:

$$\Phi_{bc}^b(j) = \Phi_{bc}^c(k) \quad (4.1.1b)$$

$$\Phi_{ca}^c(k) = \Phi_{ca}^a(i) \quad (4.1.1c)$$

Summarizing the above is the following rule for determining all triplets of indices (i, j, k) which correspond to bearings from sensors A, B , and C that mutually intersect:

Rule: The bearings from sensors A, B , and C with respective indices i, j , and k mutually intersect at the same point if and only if Eqs.(4.1.1) are satisfied.

Thus one can find the positions of the objects from bearings produced by three sensors with a common field of view by the following steps:

- (1) For each sensor, transform the spherical coordinates for each data point to the angles Φ , as defined above.
- (2) Search the sets of transformed angles, for those which satisfy Eqs. (4.1.1).
- (3) Compute the intersection location for each triplet of bearings found in step 2.

This formulation permits the use of sorting or near-neighbor algorithms to find the (i, j, k) corresponding to the same object. For example, to find those i and j satisfying Eq.(4.1.1a), combine the set $\{\Phi_{ab}^a(i)\}$ coming from sensor A with the set $\{\Phi_{ab}^b(j)\}$ from sensor B and then sort the entire set according to the values of these angles. Those angles that are equal will be near neighbors in the sorted data array and finding all such pairs will scale as N , the number of elements in the data structure. The next section describes tests on various sorting and near-neighbor methods designed to find the data satisfying Eqs.(4.1.1).

IV.2. Representative Algorithms and Tests

The algorithms and tests below account for errors in the bearing data due to finite sensor resolution. Using the notation of the previous subsection, the three sensors A , B , and C each produce bearing data transformed to the respective sets of angle pairs

$$\begin{aligned}
 \text{Sensor A : } S_a &\equiv \{(\Phi_{ab}^a(i), \Phi_{ca}^a(i)) = e_{ai} \mid i = 1, 2, \dots, N_a\} \\
 \text{Sensor B : } S_b &\equiv \{(\Phi_{ab}^b(j), \Phi_{bc}^b(j)) = e_{bj} \mid j = 1, 2, \dots, N_b\} \\
 \text{Sensor C : } S_c &\equiv \{(\Phi_{bc}^c(k), \Phi_{ca}^c(k)) = e_{ck} \mid k = 1, 2, \dots, N_c\}
 \end{aligned} \tag{4.2.1}$$

Given S_a , S_b , and S_c as input, we will examine three algorithms for finding $\Lambda \equiv \{(i, j, k) \mid \text{such that } e_{ai}, e_{bj}, e_{ck} \text{ satisfy Eq.(4.1.1)}\}$. Thus Λ is the set of index triplets that correspond to bearing vectors (one from each sensor) which intersect at the same "point" (actually a region defined by the errors of the sensors). Given the bearing vectors e_{ai} , e_{bj} , and e_{ck} , one can directly compute the coordinates (x, y, z) of the potential object.

In the tests below, the quantity ϵ denotes the characteristic error in the bearing data and is a nonzero parameter.

IV.2.1. Parallel Matching Method

This method requires two one-dimensional sorts of the angle data and thus scales as $N \ln N$. The term "parallel" here refers to the fact that the first two steps of the procedure may be performed simultaneously on a minimum of two processors. Each of the major steps of the procedure clearly contains similar searches whose lengths depends on the data sets. The degree of parallelization will depend on the architecture of the particular computer being used. The steps are as follows:

(1) Form a set, denoted S_{ab} , by combining the angles $\Phi_{ab}^a(i) \in S_a$ with the angles $\Phi_{ab}^b(j) \in S_b$. Sort S_{ab} and search outward from each element $\Phi_{ab}^a(i)$ until the difference between angle values exceeds ϵ . This gives us the following subset of S_{ab} which contains the solution along with some false solutions:

$$S_{ab}^\epsilon \equiv \left\{ S_{ab}^\epsilon(i) = \{j \mid \Phi_{ab}^a(i) - \epsilon \leq \Phi_{ab}^b(j) \leq \Phi_{ab}^a(i) + \epsilon\} \mid i = 1, 2, \dots, N_a \right\} . \quad (4.2.2)$$

(2) Perform the same operation with the angles $\Phi_{ca}^a(i) \in S_a$ and $\Phi_{ca}^c(k) \in S_c$ in a set denoted S_{ca} . This gives us the subset of S_{ca} :

$$S_{ca}^\epsilon \equiv \left\{ S_{ca}^\epsilon(i) = \{(k \mid \Phi_{ca}^a(i) - \epsilon \leq \Phi_{ca}^c(k) \leq \Phi_{ca}^a(i) + \epsilon)\} \mid i = 1, 2, \dots, N_a \right\} . \quad (4.2.3)$$

(3) Now for each i , compare all $\Phi_{bc}^b(j)$ for $j \in S_{ab}^\epsilon(i)$ with all $\Phi_{bc}^c(k)$ for $k \in S_{ca}^\epsilon(i)$. This gives us the index triplets (i, j, k) that we seek.

These subsets S_{ab}^ϵ and S_{ca}^ϵ should contain few bearings relative to the total number produced by a sensor, assuming that the sensor resolution ϵ is small relative to the average interobject angular separation. In fact, we have assumed that the subsets S_{ab}^ϵ and S_{ca}^ϵ are small relative to the binary logarithms of the number of elements in their parent sets S_{ab} and S_{ca} . Otherwise the search for the correlated elements making up set S_{ab}^ϵ , for example, would be done by constructing a binary tree containing all $\Phi_{ab}^a(i) \in S_a$ and then searching the tree for the $\Phi_{ab}^a(i)$ correlated with each $\Phi_{ab}^b(j) \in S_b$.

IV.2.2. The Monotonic Lagrangian Grid

The first step performed by the MLG method is to construct the set S_{ab}^ϵ exactly as in the parallel matching method. For each i , the angles $\Phi_{ab}^a(i) \in S_a$ and $\Phi_{ab}^b(j)$ for $j \in S_{ab}^\epsilon(i)$ will then satisfy Eq.(4.1.1a) within the accuracy defined by ϵ . Now take the set of their counterpart angles

$$S_{ab}^C \equiv \{(\Phi_{ca}^a(i), \Phi_{bc}^b(j)) \mid i = 1, 2, \dots, N_a; j \in S_{ab}^\epsilon(i)\} \quad (4.2.4)$$

and combine these pairs with their counterpart pairs $(\Phi_{ca}^c(k), \Phi_{bc}^c(k)) \in S_c$ produced by Sensor C in a two-dimensional MLG data structure:

$$\Lambda \equiv S_{ab}^C \cup S_c \quad (4.2.5)$$

The four angles satisfying the remaining two equations (4.1.1b) and (4.1.1c) should be found in proximate pairs in Λ with one pair from each of the constituent sets in Eq.(4.2.5). As noted above, when one searches small fixed-size neighborhoods of each point in the MLG, the search is rapid but some of the correlations might be missed. Thus one first finds a high percentage of the solutions, as shown by the data in Section IV.3. Then one can repeat the procedure on a much smaller data set consisting of the remaining few percent of the contact reports.

IV.2.3. A Shortcut Method

The value of this shortcut method lies in finding an acceptable percentage of possible correlations rather than all of them while reducing the amount of computation significantly. As in the previous methods, compute the set S_{ab}^ϵ defined by Eq.(4.2.4). For each i , find the element $j \in S_{ab}^\epsilon(i)$ which minimizes the deviation of $\Phi_{ab}^b(j)$ from $\Phi_{ab}^a(i)$. Then use the triplet $(\Phi_{ab}^a(i), \Phi_{bc}^b(j), \Phi_{ca}^c(i))$ as the solution. The philosophy behind this approach is that if ϵ is small, then S_{ab}^ϵ will also be small. The best value of j will then have a high likelihood of representing true correlations even without confirmation from sensor C . Thus, unlike the

MLG method which simply fails to report some correlations, the inaccuracy of the shortcut method results from the fact that some false reports may be generated. Another variation of this method might be to report every triplet $(\Phi_{ab}^a(i), \Phi_{bc}^b(j), \Phi_{ca}^c(i))$ as a correlation for $i = 1, 2, \dots, N_a$ and $j \in S_{ab}^\epsilon(i)$. This would ensure that in addition to some false reports, a report would be generated for each of the real objects observed.

IV.3. Performance Results on a SUN-260 Workstation

The following tables provide relative performance information about the three algorithms described. The tests took place on a SUN-260 Workstation, which is a scalar machine. A floating point accelerator enhanced the speed. Table 3 displays execution times and accuracy for $N_a = N_b = N_c \equiv N \in \{16K, 32K, \dots, 128K\}$ objects, with each test including an additional 10% spurious sensor readings. The value of ϵ was chosen in each test so that $\Delta^{AB}(i)$, the average number of elements in $S_{ab}^\epsilon(i)$, was approximately 1.1. Table 4 presents the results of tests performed with fixed $N = 16K$ and varying ϵ (or $\Delta^{AB}(i)$). This table reveals how the size of $S_{ab}^\epsilon(i)$ (as well as $S_{ca}^\epsilon(i)$) for the parallel matching method) affects the performance of each algorithm. Figure 4 displays the execution-time breakdown of the parallel matching and MLG methods for $N = 128K$.

The data for all tests were obtained using a random number generator $\text{rand}()$ which produces a uniform distribution of values between 0 (inclusive) and 1. The first N values for each sensor were generated as follows to ensure N correlations:

```

for  $i = 1$  to  $N$  and  $i = j = k$ ;
     $\Phi_{ab}^a(i) = \text{rand}()$ ;  $\Phi_{ab}^b(j) = \Phi_{ab}^a(i) \pm \text{rand}() \cdot \epsilon$ ;
     $\Phi_{ca}^a(i) = \text{rand}()$ ;  $\Phi_{ca}^c(k) = \Phi_{ca}^a(i) \pm \text{rand}() \cdot \epsilon$ ;
     $\Phi_{bc}^b(j) = \text{rand}()$ ;  $\Phi_{bc}^c(k) = \Phi_{bc}^b(j) \pm \text{rand}() \cdot \epsilon$ ;
end;
```

A random number of spurious readings (amounting to around 10% of N) were then added to each sensor and the order of the readings permuted so that e_{ai} , e_{bj} , and e_{ck} would not necessarily correlate for $i = j = k$. For simple statistical reasons, none of

Table 3 — Timing of Bearing Data Fusion Algorithm vs. *N*

RESULTS FOR <i>n</i> = 16,000		
Correlation Method	Time (secs)	Correlations
Parallel Matching	8.60	100.0%
MLG (offset = 1)	11.33	99.5%
MLG (offset = 2)	12.95	99.6%
MLG (offset = 3)	15.10	99.6%
Shortcut Method	3.95	98.0%

RESULTS FOR <i>n</i> = 32,000		
Correlation Method	Time (secs)	Correlations
Parallel Matching	18.47	100.0%
MLG (offset = 1)	22.48	99.6%
MLG (offset = 2)	26.43	99.7%
MLG (offset = 3)	31.32	99.7%
Shortcut Method	8.58	98.0%

RESULTS FOR <i>n</i> = 64,000		
Correlation Method	Time (secs)	Correlations
Parallel Matching	39.45	100.0%
MLG (offset = 1)	50.12	99.7%
MLG (offset = 2)	56.65	99.7%
MLG (offset = 3)	65.88	99.8%
Shortcut Method	18.32	97.9%

RESULTS FOR <i>n</i> = 128000		
Correlation Method	Time (secs)	Correlations
Parallel Matching	85.68	100.0%
MLG (offset = 1)	105.62	99.8%
MLG (offset = 2)	117.25	99.8%
MLG (offset = 3)	136.52	99.8%
Shortcut Method	39.52	98.0%

Table 4 — Timing of Bearing Data Fusion Algorithm vs. Average Data Overlap

$ \Delta^{AB}(i) = 1.1 (n = 16000)$		
Correlation Method	Time (secs)	Correlations
Parallel Matching	8.48	100.0%
MLG (offset = 1)	11.15	99.4%
Shortcut Method	3.98	98.0%

$ \Delta^{AB}(i) = 1.2 (n = 16000)$		
Correlation Method	Time (secs)	Correlations
Parallel Matching	8.79	100.0%
MLG (offset = 1)	11.34	99.4%
Shortcut Method	3.99	95.8%

$ \Delta^{AB}(i) = 1.4 (n = 16000)$		
Correlation Method	Time (secs)	Correlations
Parallel Matching	8.98	100.0%
MLG (offset = 1)	12.05	99.2%
Shortcut Method	3.98	91.8%

$ \Delta^{AB}(i) = 1.8 (n = 16000)$		
Correlation Method	Time (secs)	Correlations
Parallel Matching	9.33	100.0%
MLG (offset = 1)	13.08	99.0%
Shortcut Method	3.97	84.2%

**Execution-Time Breakdown
For n = 128,000**

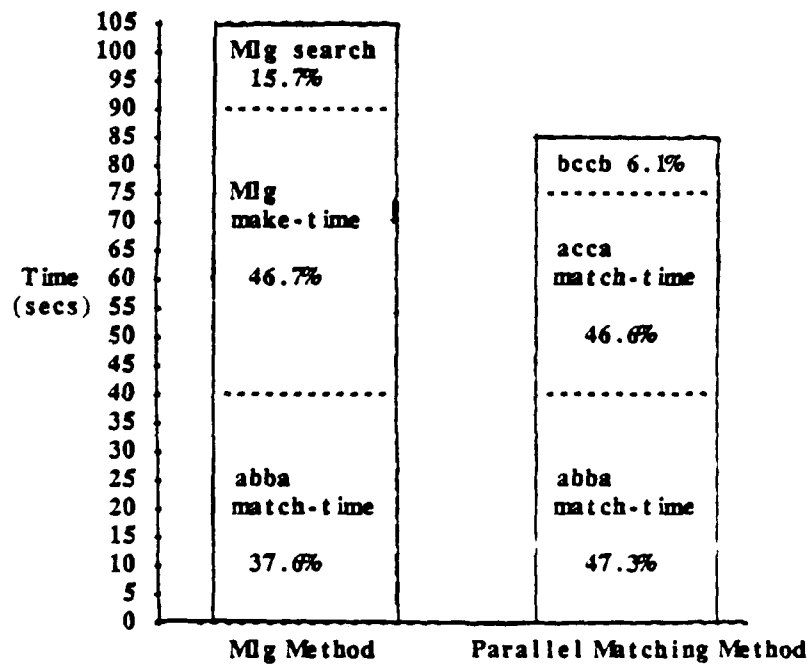


Fig. 4 — Execution time breakdowns for the MLG and the Parallel Matching Method. The notations “abba,” “acca,” and “bccb” correspond to steps 1, 2, and 3 of the latter method, respectively.

the spurious readings produced false correlations in the tests performed. To produce false correlations using these algorithms, much larger values of sensor error ϵ or many more contact reports would be required.

IV.4. Conclusions from Tests

If the accuracy of the shortcut method is acceptable for a particular application, then execution speed clearly makes it the method of choice; however, the high sensitivity to measurement error (i.e., ϵ) as target densities increase probably makes the shortcut method impractical for use in a tracking system. This being the case, the parallel matching method must be considered the superior algorithm on the SUN-260 because it is 100% accurate and faster than the MLG method. Relative to brute force algorithms, either method is much faster because of superior scaling with the size of the data set.

IV.5 Estimates of Performance on Other Hardware

Table 5 gives estimates of the performance of our multisensor fusion algorithm on various machines, both sequential and parallel. The numbers are based on tests using the MLG and on relative speeds of the computers. Under each machine name is the source of the estimate. The timing estimates shown correspond to 32,000 objects as viewed by the three sensors. On various vector and parallel machines, the processing time is on the order of 1 cpu second. The algorithm has thus reduced the complexity of the problem to the point at which existing hardware can process the data rapidly for large numbers of objects. With expected improvements in processing speed over the next few years, data processing systems should easily meet the requirements for bearing to position conversion on large numbers of objects with realistic values of sensor false alarm and error rates.

Table 5 — Estimates of Performance of Bearing Data Fusion Algorithm on Various Hardware

Multisensor Fusion -- Angle-to-Position Conversions Timings for 32,000 Objects Seen by Three Sensors

<u>Computer System</u>	<u>Size scaling</u>	<u>Timing in Seconds Present</u>	<u>Timing in Seconds Possible</u>
DEC VAX 11/780 (FP accelerator) (2,000+ objects in 5.6 sec)	$N \log_2 N$	100	60
DEC VAX 8800 (FP accelerator) (estimated 5 x VAX 11/780)	$N \log_2 N$	20	12
Scientific Computer Systems 40 (estimated at 0.3 Cray XMP)	$N \log_2 N$	9	3
APTEC IOC 24 - 3 N432s (measured, 30 VAX 11/780)	$N/M \log_2 N$	4	1.5
Cray X-MP (1 processor of 4) (2,000 objects in 0.17 sec)	$N \log_2 N$	3	1.2
16K Alpha Connection Machine (8,000 element sorts)	$\log_2 N$	1.0	0.6
CRAY X-MP (4 processors of 4) (estimated 3 x 1 processor)	$N \log_2 N$	1.0	0.4
APTEC IOC 200 - 10 XAP boards (measured, 25 VAX 11/780)	$N/M \log_2 N$	1.0	0.4
64K Beta Connection Machine (linear + improvements)	$\log_2 N$	0.3	0.2

V. Summary

This report has presented a preliminary view of the use of near-neighbor algorithms in the processing of data on the bearings of the objects being observed. By assumption, the sensors, such as infrared imaging devices, have provided either poor range information or none at all. Our orientation has been toward correlation and tracking of large numbers of high-speed objects. The purpose of the near-neighbor algorithms has been to organize the data on a set of objects to permit rapid access of the data with a high correlation to a given member of another set. The combinatorially inefficient "brute force" method, in which all possible correlations between the two sets are considered, provides a baseline for assessing the performance of the near-neighbor techniques. An interesting realization is that, although the NN algorithms permit actual access to be superior, the overall cost of the NN approach could be greater than brute force. This occurs, for example, if the NN data structure must be set up too frequently. If the same data structure can be used for groups of contact reports, then the NN algorithms should be much faster.

Some near-neighbor algorithms are also imperfect in that some near-neighbors, by whatever definition of "nearness," might be missed if the search is too restricted. Clustering algorithms can permit ambiguous assignments of objects to particular clusters, for example. The MLG algorithm can require searches of irregular regions of index space or of large regions in order to insure finding all of the near neighbors. Tree-like searches of the MLG data structure [6] might be necessary in some cases.

We have described the manner in which NN algorithms can be used in correlating bearing data from a given sensor with a group of three-dimensional tracks. This is straightforward, and appropriate test results on data access in this situation are available¹ for the MLG and Hockney's method.

The paper has also presented an example of a high-speed algorithm for converting multisensor bearing data to positions for the objects within the region common to all of the sensors. These algorithms will be superior to any brute force method for three or

more sensors, since the latter scales as N^m , where m is the number of sensors, while our algorithm is particularly suited for NN algorithms, which scale as $N \ln N$. The algorithm also reduces the problem from determining the m -fold intersections of lines to the pairwise equality of special angles. Thus the complexity is greatly reduced. Performance tests and estimates indicate that the algorithms might already give existing hardware the capability to satisfy the estimated processing requirements for situations in which large numbers of objects are moving at high speeds. Certainly this will be the case in the future, given the anticipated improvements in speed and memory of computer hardware.

VI. Acknowledgements

The authors acknowledge the support of the Strategic Defensive Initiative Organization and the Defense Advanced Research Projects Agency for the development of the ideas presented in this paper. We also appreciate the effort of J. V. W. Reynders in programming an initial version of the multisensor fusion algorithm on the Thinking Machines Corporation Connection Machine.

References

1. J. A. Erbacher and B. Belkin, *Tracker/Correlator Algorithm Design Document* (Ball Systems Engineering Division, Arlington, Virginia, 1988).
2. S. S. Blackman, *Multiple-Target Tracking with Radar Applications* (Artech House, Dedham, Massachusetts, 1986).
3. J. M. Picone, M. Zuniga, and J. Uhlmann, *Tests of Gating Algorithms for Tracking of Multiple Objects I. Theory, Requirements, and Performance Measures*, NRL Memorandum Report, to be submitted (1989).
4. R. W. Hockney and J. W. Eastwood, *Computer Simulation Using Particles*, McGraw-Hill, New York, chapter 8, pp. 267-309 (1981).
5. J. P. Boris, "A Vectorized 'Near Neighbors' Algorithm of Order N Using a Monotonic Logical Grid", *J. Comp. Phys.* **66**(1), PP. 1-20 (1986).
6. B. S. Kim and S. B. Park, "A Fast k -Nearest-Neighbor-Finding Algorithm Based on the Ordered Partition", *IEEE Transactions on Pattern Analysis and Machine Intelligence*, Vol. PAMI-8, No. 6, pp.761-766 (1986).
7. R. Varad, private communication, MITRE Corp., Bedford, Massachusetts (1989).

Appendix: Details of Multisensor Bearing-to-Position Conversion

For completeness, this appendix gives details on the transformation of the bearing data from each sensor to new angles denoted by Φ . Figure 5 returns to the example used previously (Fig. 3) for a bearing vector e_{bj} corresponding to Sensor B. Figure 5b shows that the angle $\Phi_{bc}^b(j)$ can be computed from the unit normals to the plane of the sensors and the plane defined by e_{bc} (the vector from Sensor B to Sensor C) and the bearing vector e_{bj} .

First define the unit vector β_s perpendicular to the plane of the sensors. If the site producing the bearing vector is $l \in \{A, B, C\}$, then we define the values of $l-1$ and $l+1$ by the preceding and following sensor indices in the appropriate cyclic permutation of the sequence $A-B-C$. For example, if $l = B$, then $l-1 = A$ and $l+1 = C$. Then the desired unit vector is the vector cross product

$$\beta_s \equiv \frac{e_{l(l+1)} \times e_{(l-1)l}}{|e_{l(l+1)} \times e_{(l-1)l}|} \quad (A.1)$$

In our example with $l = B$, this becomes

$$\beta_s \equiv \frac{e_{bc} \times e_{ab}}{|e_{bc} \times e_{ab}|} \quad (A.2)$$

The perpendicular to the plane \overline{BCj} is

$$\beta_{bc}(j) \equiv \frac{e_{bj} \times e_{bc}}{|e_{bj} \times e_{bc}|} \quad (A.3)$$

The angle $\Phi_{bc}^b(j)$ then satisfies the equations

$$\sin \Phi_{bc}^b(j) \equiv (\beta_{bc}(j) \times \beta_s) \cdot e_{bc} \quad (A.4a)$$

$$\cos \Phi_{bc}^b(j) \equiv \beta_{bc}(j) \cdot \beta_s \quad (A.4b)$$

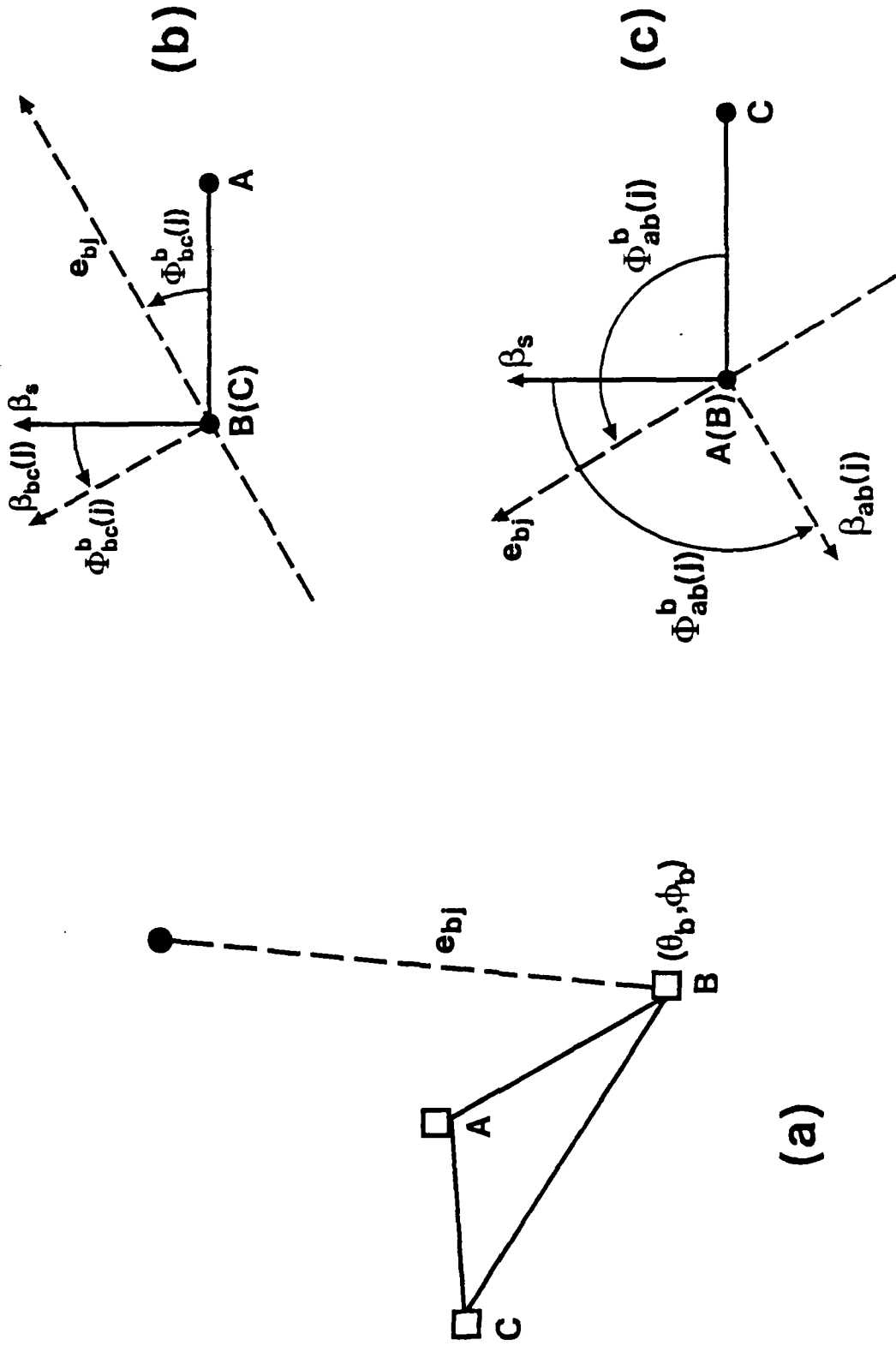


Fig. 5 — Same as Figure 3 but with more detail, including the definitions of the normal vectors “ β ” to the planes and their use in defining the transformed angles Φ .

in which the centered dot (\cdot) signifies a scalar product. Figure 5c shows the definition of the second angle $\Phi_{ab}^b(j)$ corresponding to the bearing vector e_{bj} . This is the angle between the plane of the sensors and the plane defined by the line joining sensors A and B and the bearing vector e_{bj} . By convention (Section IV.1), the observer's line of sight runs from sensor A toward sensor B , producing the view shown in Fig. 5c. A cyclic permutation of the subscripts $A - B - C$ will define the angles corresponding to bearing vectors produced by sensors A and B .

The remaining question is that of transforming the uncertainty $(\Delta\theta, \Delta\phi)$ to uncertainties in the new angles Φ . Again consider the angle $\Phi_{bc}^b(j)$ and the bearing vector $e_{bj} \equiv (\theta_b(j), \phi_b(j))$. Define the right-handed coordinate axes (visualize with Fig.5b)

$$\begin{aligned} x &\equiv e_{bc} \\ y &\equiv e_{ab} \\ z &\equiv \beta_s \end{aligned} \tag{A.5}$$

Then, if the subscripts on the bearing angles are dropped for convenience, the important unit vectors are

$$\begin{aligned} e_{bj} &= (\sin \theta \cos \phi, \sin \theta \sin \phi, \cos \theta) \\ \beta_s &= (0, 0, 1) \\ e_{bc} &= (1, 0, 0) \end{aligned} \tag{A.6}$$

Equation(A.3) then gives us

$$\beta_{bc}(j) = G(0, \cos \theta, -\sin \theta \sin \phi), \tag{A.7}$$

where

$$G = (\cos^2 \theta + \sin^2 \theta \sin^2 \phi)^{-\frac{1}{2}}. \tag{A.8}$$

Equations(A.4) then become

$$\begin{aligned}\sin \Phi_{bc}^b(j) &= G \cos \theta \\ \cos \Phi_{bc}^b(j) &= -G \sin \theta \sin \phi\end{aligned}\tag{A.9}$$

Equations (A.7)-(A.9) show that the error in the new angles varies with the bearing vector e_{bj} . The new angles themselves can become undefined for pathological cases in which the three bearing vectors are not distinct or for which the bearing vectors lie close to the plane of the sensors. An example would be an object lying along or near the line e_{bc} , in which case $(\theta, \phi) = (\frac{\pi}{2}, 0)$. At the other extreme, for $\theta = m\pi$, where m is an integer, and variable ϕ , the error in $\Phi_{bc}^b(j)$ is $\Delta\Phi^2 \sim \Delta\theta^2$. The general equations for the error become unwieldy because of the normalization factor G . A detailed examination is necessary to determine the ranges of bearing vectors for which their intersections yield useful position data. Since our method is equivalent to the brute force ("intersection") approach, the range of validity will be the same. One method of determining this range in the context of our method is to use the equations in this appendix in conjunction with a limit on the allowable size of the errors in the angles Φ . An example of such a constraint is

$$(\Delta\Phi_{bc}^b(j))^2 < (\Delta\theta + \Delta\phi)^2.\tag{A.10}$$